DEVELOPMENT OF PALLADIUM IMPREGNATED TITANIA MEMBRANE TO ENHANCE HYDROGEN PERMEABILITY

MUHAMMAD AZAN BIN TAMAR JAYA

UNIVERSITI SAINS MALAYSIA

2011

DEVELOPMENT OF PALLADIUM IMPREGNATED TITANIA MEMBRANE TO ENHANCE HYDROGEN PERMEABILITY

by

MUHAMMAD AZAN BIN TAMAR JAYA

Thesis submitted in fulfillment of the requirements for the degree of Master of Science

JULY 2011

ACKNOWLEDGEMENTS

First and foremost, a great thankful to God, Allah S.W.T. for blessing me, giving me strength, good health and make my life easier until I finished my study. A special gratitude to my beloved parents, Mr. Tamar Jaya Nizar, and Mrs. Salmah Ali, and also to all my family members for their endless support and prays.

I would like to take this opportunity to express a special thank to my supervisor, Prof. Abdul Latif Ahmad for his excellent knowledgeable guidance, encouragement, invaluable suggestion, assistance, and advises rendered throughout my research. With his advice and support during my research period, I'm able to complete this thesis completely. Also, I would like to express my gratitude to my co-supervisor, Dr. Derek Chan Juinn Chieh for sharing his knowledge, opinion and helping me throughout the research.

Not forgetting, thanks a lot to all technicians and staffs of School of Chemical Engineering for their cooperation and warmest helping hand. Deepest thank to all my beloved friends for the help, for the moral support and for encouraging me throughout this study.

Last but not least. I would like to give a special thank to whom has helped and contributed either directly or indirectly in completing my research. Without a well warm cooperation from all of you I would not be successful to come out with this thesis. Thank you very much.

TABLE OF CONTENTS

ACKNOWLEDGEMENTS		ii
TABLE OF CONTENTS		iii
LIST OF TABLES		viii
LIST OF FIGURES		x
LIST OF PLATES		xiii
LIST OF SYMBOLS		xv
LIST OF ABBREVIATION		xvii
ABSTRAK		xix
ABSTRACT		xxi
CHAPTER 1: INTRODUCTION		1
1.0	Membrane technology	1
1.1	Problem statement	4
1.2	Research objective	8
1.3	Organization of the thesis	8
CHAPTER 2: LITERATURE REVIEW		10
2.0	Development of TiO_2 membrane	10
2.1	Development of Palladium (Pd) based membrane	16
2.2	Sol-gel and membrane formation	18
	2.2.1 Effect of peptizing agent	21
	2.2.2 Effect of sol concentration	23
	2.2.3 Effect of binder	24
2.3	Unsupported membrane analysis	26
	2.3.1 X-ray diffraction (XRD) analysis	26
	2.3.2 N_2 adsorption/desorption analysis	27

2.3.3 Surface fractal analysis 30

2.3.4 Effect of peptizing agent 32

2.3.5 Effect of calcination temperature 33

2.3.6 Effect of phase transition 36

2.3.7 Effect of metal addition 37

2.4 Supported membrane analysis 39

2.4.1 Performance evaluation 39

2.4.2 Membrane separation mechanism 42

2.4.2 (a) Effect of operating pressure and temperature 45

2.4.2 (b) Effect of metal addition 47

CHAPTER 3: METHODOLOGY 48

3.0 Introduction 47

3.1 Chemicals 49

3.2 Experimental method 50

3.2.1 Preparation of titania sol 50

3.2.2 Preparation of palladium chloride ($PdCl_2$) solution 51

3.2.3 Preparation of HPC and PVA solution 51

3.2.4 Preparation of titania sol for coating 52

3.3 Preparation of membrane 53

3.3.1 Preparation of membrane support 53

3.3.2 Preparation of supported membrane 54

3.3.3 Preparation of unsupported membrane 54

3.4 Characterization analysis 55

3.5 Sample preparation for characterization 57

3.6 Characterization 58

3.6.1 Effect of H^+/Ti^+ molar ratio 58

3.6.2 Effect of calcination temperature 59

3.6.3 Effect of sol concentration 60

3.6.4 Effect of binder concentration 60

3.6.5 Binder decomposition study 61

3.6.6 Effect of palladium addition 62

3.6.7 Permeability and permselectivity test 63

CHAPTER 4: RESULTS AND DISCUSSION 66

4.0 Introduction 66

4.1 Characterization of membrane support 66

4.2 Effect of H^+/Ti^{4+} molar ratio 71

4.2.1 Effect on sol appearance and stability 72

4.2.2 Effect on membrane morphology 76

4.2.3 Effect on TiO_2 membrane crystal structure 82

4.3 Effect of calcination temperature 87

4.3.1 Effect on TiO_2 membrane crystal structure 87

4.3.2 Effect of rutile presence on TiO_2 membrane pore structure 90

4.4 Effect of sol concentration 93

4.5 Effect of binder 99

4.5.1 Effect on sol turbidity 100

4.5.2 Effect on membrane morphology 103

4.5.3 Effect on TiO_2 membrane pore structure 106

4.5.4 Binder decomposition 107

4.5.4 (a) Thermogravimetric analysis of unsupported Pd-TiO_2 membrane 107

4.5.4 (b) Fourier Transform Infra Red (FTIR) 110

4.6 Palladium impregnation 112

4.6.1 Effect on TiO_2 membrane crystal structure 113

4.6.2 Effect of Pd on TiO_2 membrane pore structure 116

4.6.3 Surface fractal analysis 122

4.6.4 Effect of binders on Pd-TiO_2 membrane crystal structure 123

4.6.5 Energy Dispersive X-ray (EDX) analysis 127

4.7 Permeability and permselectivity evaluation 131

4.7.1 TiO_2 membrane 132

4.7.1 (a) Effect of operating pressure and temperature on permeability of TiO_2 membrane 132

4.7.1 (b) Effect of operating pressure and temperature on permselectivity of TiO_2 membrane 135

4.7.2 Pd-TiO_2 membrane 138

4.7.2 (a) Effect of operating pressure and temperature on permeability of Pd-TiO_2 membrane 138

4.7.2 (b) Effect of Pd loading on permselectivity of Pd-TiO_2 membrane at different operating pressure and temperatures 141

CHAPTER 5: CONCLUSIONS AND RECOMMENDATIONS 145

5.1 Conclusions 145

5.2 Recommendations 148

REFERENCES 150

APPENDICES 162

Appendix A 162

Appendix B 163

Appendix C 165

Appendix D 168

List of publications, seminars and awards 170

LIST OF TABLES

		Page
Table 2.1	Membrane sample and its respective measured surface roughness (Chou et al., 1999)	14
Table 2.2	Relation between grain size and surface area when the calcination temperature of TiO_2 is increased (Liu et al., 2002)	35
Table 2.3	The fundamental structural unit of TiO_2 crystal phases (Watson et al. 2004)	36
Table 2.4	BET surface area of metal doped samples (Nagaveni et al. 2004	38
Table 2.5	Gas separation using ceramic membranes (Mallada & Menendez, 2008)	43
Table 3.1	List of chemicals used in conducting the experiment	50
Table 3.2	Equipment/ analysis used for the project	55
Table 3.3	Different points of sample taken for FTIR analysis	62
Table 4.1	Surface roughness parameters of membrane support and supported Pd-TiO_2 membrane	68
Table 4.2	Pore structure of membrane support	70
Table 4.3	Sol appearance affected by different H^+/Ti^{4+} molar ratio	73
Table 4.4	The effect of molar ratio on anatase percentage and its crystallite size	84
Table 4.5	Membrane appearance after coating with different sol concentration	94
Table 4.6	Effect of different combination of PVA and HPC on turbidity changes of titania sol and the formation of crack-free supported membrane	103
Table 4.7	The effects of binders addition on TiO_2 unsupported membrane morphology	107
Table 4.8	Color observation on unsupported TiO_2 membrane sample at different temperature during calcination	109
Table 4.9	Sample name for different Pd concentration of supported/ unsupported Pd-TiO_2 membrane	113
Table 4.10	Effect of Pd on TiO_2 crystallite size	116

Table 4.11	Estimated crystallite size corresponding to palladium content and binders	126
Table 4.12	Weight and Atomic percentage based on EDX measurement on *AREA1*	129
Table 4.13	Gas molecular properties (Othman and Kim, 2008)	135

LIST OF FIGURES

Figure 1.1	Schematic representation of membrane process	1
Figure 2.1	Schematic flow diagram of colloidal and polymeric routes in sol-gel process	20
Figure 2.2	Type of adsorption isotherms (BDDT classification) (Miyahara, 2007)	27
Figure 2.3	Types of hysteresis loop classified by de Boer (Igwe, 1991)	28
Figure 2.4	Schematic flow diagram of membrane test rig for permeation experiment (Pizzi et al., 2008)	40
Figure 2.5	Transport mechanisms for different types of membrane with its corresponding theoretical selectivity	44
Figure 3.1	Schematic flow diagram of the whole project	49
Figure 3.2	Schematic flow diagram of the preparation of titania sol	52
Figure 3.3	Schematic low diagram of preparing supported and unsupported membrane	53
Figure 3.4	Sintering temperature profile for unsupported and supported membrane	55
Figure 3.5	Schematic flow diagram of permeation test rig	64
Figure 4.1	AFM images of surface of membrane support and supported Pd-TiO_2 membrane taken at 30.00 x 30.00 µm	68
Figure 4.2	Pore width distribution of membrane support	71
Figure 4.3	XRD pattern of TiO_2 calcined at 400^oC from titania sol with different H^+/Ti^{4+} molar ratio	83
Figure 4.4	XRD patterns of unsupported TiO_2 membranes at different calcination temperatures synthesized using titania sol with 0.5 H^+/ti^{4+} molar ratio	88
Figure 4.5	XRD patterns of unsupported TiO_2 membranes at different calcination temperatures synthesized using titania sol with 0.1 H^+/Ti^{4+} molar ratio	90
Figure 4.6	N_2 adsorption/desorption isotherm of unsupported TiO_2 membrane calcined at 500^oC	91
Figure 4.7	Pore width distribution of unsupported TiO_2 membrane calcined at 500^oC	92

Figure 4.8	Turbidity changes of titania sol at different concentration of PVA and HPC	101
Figure 4.9	Pore width distribution of TiO_2 unsupported membrane of low (LBC) and high binder concentration (HBC)	107
Figure 4.10	TG/DTA curves of Pd-TiO_2 xerogel under normal atmosphere	108
Figure 4.11	FTIR spectras of unsupported TiO_2 membrane at different temperature	111
Figure 4.12	XRD patterns of unsupported TiO_2 and Pd-TiO_2 membrane sintered at 400^oC	114
Figure 4.13	XRD patterns of unsupported Pd-TiO_2 membrane sintered at 500^oC	115
Figure 4.14	Pore width distribution and isotherm plot of an unsupported TiO_2 membrane calcined at 400^oC	116
Figure 4.15	Pore width distribution and isotherm plot of an unsupported Pd_2-TiO_2 membrane calcined at 400^oC	117
Figure 4.16	Pore width distribution and isotherm plot of an unsupported Pd_6-TiO_2 membrane calcined at 400^oC	117
Figure 4.17	Pore width distribution and isotherm plot of an unsupported Pd_{10}-TiO_2 membrane calcined at 400^oC	117
Figure 4.18	Effect of different Pd concentration on BET surface area	120
Figure 4.19	Effect of different Pd concentration on pore volume	121
Figure 4.20	Effect of different Pd concentration on average pore width	122
Figure 4.21	Effect of Pd loading on surface fractal dimension	123
Figure 4.22	XRD patterns for TiO_2 that contained different concentrations of Pd^{2+}, with and without binders	124
Figure 4.23	EDX profile for *AREA1* (refer Plate 4.19(a)	129
Figure 4.24	EDX profile for *spot2* (refer Plate 4.17(b)	130
Figure 4.25	H_2 and N_2 permeability of three operating pressures across the TiO_2 membrane at different temperatures	133
Figure 4.26	H_2 and N_2 permeability in a function of operating pressures	134
Figure 4.27	H_2 and N_2 permselectivity of three operating pressures across the TiO_2 membrane at different temperatures	136

Figure 4.28	Permselectivity of H_2/N_2 across TiO_2 membrane in a function of operating pressures	138
Figure 4.29	Permeability of H_2 and N_2 across Pd-TiO_2 membranes with different concentrations of Pd at operating pressure of 1 bar	139
Figure 4.30	Permeability of H_2 and N_2 across Pd-TiO_2 membrane in a function of operating pressures	141
Figure 4.31	Mean permselectivity (H_2/N_2) of Pd-TiO_2 membranes in a function of Pd concentration, temperature, and operating pressure	142

LIST OF PLATES

Plate 4.1	SEM image of membrane support top surface taken at 1000 mag and 20000 mag (inset)	69
Plate 4.2	Cross-sectional SEM image of membrane support taken at 1000 mag and 10000 mag (inset)	70
Plate 4.3	Titania colloidal sol of 0.5 H^+/Ti^{4+} molar ratio viewed through TEM	75
Plate 4.4	SEM cross-sectional view of supported Pd_2-TiO_2 membrane with 4 coatings at 2.5 H^+/Ti^{4+} molar ratio taken at 5000 mag	77
Plate 4.5	SEM view of top surface of supported Pd_2-TiO_2 membrane with 4 coatings at 2.5 H^+/Ti^{4+} molar ratio taken at 5000 mag	78
Plate 4.6	SEM cross-sectional view of supported Pd_2-TiO_2 membrane with 8 coatings at 2.5 H^+/Ti^{4+} molar ratio taken at 2000 mag	79
Plate 4.7	SEM top view of supported Pd_2-TiO_2 membrane with 8 coatings at 2.5 H^+/Ti^{4+} molar ratio taken at 2000 mag	79
Plate 4.8	SEM cross-sectional view of supported Pd_2-TiO_2 membrane with 4 coatings at 1.0 H^+/Ti^{4+} molar ratio taken at 500 mag	80
Plate 4.9	SEM top view of supported Pd_2-TiO_2 membrane with 4 coatings at 1.0 H^+/Ti^{4+} molar ratio taken at 1000 mag	80
Plate 4.10	The top view of SEM image of supported Pd-TiO_2 membrane with coating at 0.5 H^+/Ti^{4+} molar ratio taken at 100 mag and 3000 mag (inset)	81
Plate 4.11	SEM cross-sectional view of supported Pd-TiO_2 membrane with coating at 0.5 H^+/Ti^{4+} molar ratio taken at 3000 mag with larger 15000 mag shown by the inset	82
Plate 4.12	TEM image of TiO_2 microstructure at H^+/Ti^{4+} molar ratio of a-b)0.5, c-d) 1.5, e-f)2.5, g-h)3.5; where a, c, e, and g are viewed at 185K mag; b,d,f and h are viewed at 600K mag	86
Plate 4.13	Light microscope image of sol deposited on membrane support taken at 200x mag after calcination using sol concentration of (a) 0.2 mol Ti^{4+}/dm^3 (b) 0.1 mol Ti^{4+}/dm^3 (c) 0.05 mol Ti^{4+}/dm^3 (d) 0.025 mol Ti^{4+}/dm^3	95
Plate 4.14	Cross-sectional SEM image of supported TiO_2 membrane synthesized by sol concentration of 0.013 mol Ti^{4+}/dm^3 taken at 3000 mag with a larger 10000 mag shown by the inset	95

Plate 4.15	Light microscope image of sol deposited on glass substrates taken at 400x mag after calcination using sol concentration of (a) 0.2 mol Ti^{4+}/dm^3 (b) 0.1 mol Ti^{4+}/dm^3 (c) 0.05 mol Ti^{4+}/dm^3 (d) 0.025 mol Ti^{4+}/dm^3 with enlarged images for clearer view in (c) and (d)	97
Plate 4.16	Dried gel without any addition of binders on membrane support before sintering process	105
Plate 4.17	Top of SEM image of a sintered membrane with the aid of binders on a membrane support	105
Plate 4.18	Agglomeration emerges on supported Pd-TiO_2 membrane after reduction treatment	128
Plate 4.19	EDX measurement on Pd-TiO_2 membrane based on a) area *AREA1* and b) spot *spot2*	128
Plate 4.20	EDX mapping of a) Pd-TiO_2 supported membrane indicating that the existence of elemental b) Ti, c) O, and d) Pd	131

LIST OF SYMBOLS

γ	gamma
A_m	Membrane's effective surface area (m^2)
I_A	highest integrated peak intensities of anatase
I_R	highest integrated peak intensities of rutile
L_m	Thickness of membrane (m)
Q_i	Volumetric flow rate of gas i ($m^3.s^{-1}$)
X_A	The mass fraction of anatase
p/p_o	Relative pressure
$\bar{p}$	Average pressure across the membrane (Pa)
p_h	Upstream pressure (Pa)
p_l	Downstream pressure (Pa)
p_o	Saturation pressure (Pa)
r_K	Kelvin radius (nm)
r_p	Pore radius (m)
q	Amount adsorbed (Pa)
r_n	Radii of the narrow parts (m)
r_w	Radii of the wide parts (m)
T	Temperature (K)
α	permselectivity
D	Crystallite size (nm)
J	Gas flow rate ($mol.s^{-1}$)
L	Length of membrane tube (m)
N	Avogadro number
P	Pressure difference across membrane (Pa)
R	Gas constant ($m^3.Pa.K^{-1}.mol^{-1}$)
V	molar volume of the liquid (m^3mol^{-1})

dP	Difference in partial pressure (Pa)
k	Constant of 0.9
p	Applied pressure (Pa)
r	Outer radius of membrane tube (m)
t	Thickness (m)
β	FWHM (rad)
θ	Angle (°)
λ	X-ray wavelength (Å)
λ	Mean free path (m)
π	Permeability ($mol.m.s^{-1}.m^{-2}.Pa^{-1}$)
σ	surface tension of the liquid condensate (Nm^{-1})

LIST OF ABBREVIATIONS

AFM	Atomic Force Microscope
APCVD	Atmospheric pressure chemical vapor deposition
BDDT	Brunauer-Deming-Deming-Teller
BET	Brynauer-Emmet-Teller analysis
CVD	Chemical vapor deposition
DEA	Diethanol-amine
DTA	Differential thermal analysis
ED	Electrodialysis
EDX	Energy-dispersive d x-ray
FHH	Frankel-Halsey-Hill method
FTIR	Fourier Transform Infra-Red
FWHM	Full width at half maximum
GLM	General Linear Model
H_2O_2	Hydrogen peroxide
HPC	Hydroxyl-propyl cellulose
ITO	Indium tin oxide
IUPAC	The International Union of Pure and Applied Chemistry
LM	Light microscope
LPD	Liquid phase deposition method
MF	Microfiltration
NF	Nanofiltration
PAM	Polyacrylamide
Pd-TiO_2	Palladium-titania membrane
Pd_x-TiO_2	Palladium-titania membrane with *x* concentration of Pd (*x* = 2, 6, 10, 15, 20)
PEG	Polyethylene glycol

PEI	Polyethyleneimine
PVA	Polyvinyl alcohol
PVDF	Polyvinylidene fluoride
RO	Reverse osmosis
SEM	Scanning electron microscope
TCM	Tubular catalytic membrane
TEM	Transmission electron microscope
TGA	Thermogravimetric analysis
TiO_6^{2-}	Titanium octahedron
$Ti(O\text{-}n\text{-}Bu)_4$	Tetra-n-butyl titanate
TTIP	Titanium tetra-isopropoxide
UF	Ultrafiltration
WPS	Wet powder spraying method
XRD	X-ray diffraction
Y_2O_3	Yttria
YSZ	Yttria-stabilized zirconia

PEMBANGUNAN MEMBRAN TITANIA BERIMPRAGNASIKAN PALLADIUM UNTUK MENINGKATKAN KEBOLEHTELAPAN HIDROGEN

ABSTRAK

Kajian ini dijalankan untuk membangunkan membran seramik yang telah digabungkan dengan elemen paladium yang mempunyai kadar afiniti yang tinggi terhadap gas hidrogen untuk meningkatkan tahap kememilihan. Bagi mengekalkan kadar kebolehtelapan pada tahap yang tinggi, seramik TiO_2 telah dipilih atas dasar tahap tortuositinya yang rendah. Kajian ini memfokuskan pada sintesis dan pencirian membran TiO_2 berimprignasikan paladium (membran Pd-TiO_2) dengan kaedah sol-gel. Penambahan elemen paladium pada membran TiO_2 dilakukan dengan kaedah pencampuran sol titania dengan larutan prapenanda Pd. Struktur mikro dan morfologi membran telah dicirikan dan dianaisa menggunakan analisis Belauan Sinar-X (XRD),Mikroskop Elektron Imbasan Pancaran Medan (SEM), Mikroskop Elektron Transmisi (TEM), Permeteran Gravity (TGA), Penjelmaan Infra Merah Fourier (FTIR), Penyeberan Energi Sinar-X (EDX), Penjerapan Nitrogen, dan Mikroskop Gaya Atom (AFM). Kesan beberapa parameter penting dalam usaha mendapatkan membran Pd-TiO_2 yang bebas-retakan telah dikaji secara mendalam. Parameter-parameter tersebut adalah kesan nisbah molar H^+/Ti^{4+}, suhu pembakaran, kepekatan sol, pelekat dan paladium. Kadar optima untuk nisbah molar H^+/Ti^{4+} adalah 0.5. Pada nisbah ini, sol yang terhasil didapati lebih stabil dalam jangka masa yang panjang selain memberikan kualiti salutan yang baik. Dari segi pembakaran, fasa transisi daripada “antase” kepada “rutile” bermula setelah suhu mencecah 400^oC. Kepekatan sol juga didapati memberikan kesan ke atas penghasilan membran seramik TiO_2 yang bebas-retakan dimana kepekatan sol yang tinggi menyebabkan membran menjadi retak setelah pengkalsinan. Penggunaan lekatan telah berjaya diminimumkan tanpa

menyebabkan sebarang retakan setelah pengkalsinan. Selain itu, penambahan pelekat juga didapati memberikan kesan kepada struktur liang membran. Berdasarkan analisis TGA dan FTIR, tiada tinggalan pelekat yang dapat dikesan pada membran Pd-TiO_2 setelah suhu pengkalsinan mencecah 400^oC. Kesan impregnasi Pd pada membran TiO_2 telah dikaji dengan teliti. Berdasarkan analisis XRD, kehadiran Pd telah merencatkan tumbesaran kristal dan fasa transisi daripada "anatase" kepada "rutile". Penambahan Pd juga mengakibatkan kenaikan yang signifikan pada luas permukaan, isipadu dan saiz liang membran TiO_2 di tahap keliangan meso. Selain itu, taburan saiz liang membentuk dwi-modal dimana bilangan saiz liang sekunder meningkat apabila kepekatan Pd ditingkatkan. Analisis permukaan fraktal menunjukkan kehadiran Pd telah menyebabkan kekasaran membran TiO_2 bertambah. Berdasarkan gambar SEM, ketebalan membran adalah kurang daripada 1 μm. Mekanisma pengangkutan bagi membran Pd-TiO_2 secara hampir keseluruhannya dipengaruhi oleh resapan Knudsen and aliran Poiseulle dengan peningkatan kadar kebolehtelapan berbanding membran TiO_2. Fenomena ini adalah selari dengan keputusan daripada analisis Penjerapan Nitrogen. Kadar kebolehtelapan gas H_2 dan N_2 menunjukkan penurunan yang ketara apabila suhu operasi ditingkatkan daripada suhu bilik ke 350^oC tetapi menunjukkan peningkatan apabila tekanan operasi ditingkatkan. Walaubagaimanapun, kadar pemisahan-penelapan menurun apabila tekanan operasi ditingkatkan tetapi menunjukkan kenaikan berkala apabila suhu operasi dinaikkan. Dari segi kepekatan Pd, kadar pemisahan-penelapan adalah tertinggi pada kadar penambahan Pd sebanyak 10 w/w%. Sebagai kesimpulannya, proses impregnasi Pd mampu memberikan peningkaatan pada membran TiO_2 dari segi kadar kebolehtelapan dan pemisahan-penelapan.

DEVELOPMENT OF PALLADIUM IMPREGNATED TITANIA MEMBRANE TO ENHANCE HYDROGEN PERMEABILITY

ABSTRACT

The current study has been conducted to develop a ceramic membrane combined with palladium metal that offers great affinity towards hydrogen to improve the selectivity. In order to obtain the highest permeability, TiO_2 ceramic which has low tortuosity compared to other ceramic materials was utilized. The study focused on the synthesis and characterization of TiO_2 membrane with the impregnation of elemental palladium (Pd-TiO_2 membrane). The introduction of Pd element into the TiO_2 membrane was done by sol-mixing between the titania sol and Pd precursor solution. The membrane microstructure and morphology were analyzed using X-ray Diffraction (XRD), Scanning Electron Microscopy (SEM), Transmission Electron Microscopy (TEM), Thermal Gravimetric analysis (TGA), Fourier Transform Infra Red (FTIR) analysis, Energy Dispersive X-ray (EDX), N_2 adsorption/desorption, and Atomic Force Microscopy (AFM). The effects of several important parameters to obtain a crack-free Pd-TiO_2 membrane were thoroughly investigated which were the effect of H^+/Ti^{4+} molar ratio, calcination temperature, sol concentration, binders, and palladium concentration. The optimum molar ratio of H^+/Ti^{4+} was found to be 0.5. At this level, the produced sol was found to be stable for a very long period of time with the best performance in coating. In term of thermal treatment, the phase transition of anatase to rutile began after 400^oC. Sol concentration was also found to affect the production of crack-free Pd-TiO_2 membrane where higher sol concentration caused the membrane to crack after calcination. Binder usage has been successfully minimized without causing the membrane to crack after calcination. It was found that, addition of binders did not only produce a crack-free membrane but also

affected the membrane pore structure. According to TGA and FTIR analysis, no trace of binders was detected in the Pd-TiO_2 membrane when the calcination temperature reaches 400^oC. The impact of Pd impregnation into the TiO_2 membrane has been extensively investigated. Based on XRD analysis, the presence of Pd has retarded the crystal growth and phase transition of anatase to rutile. The addition of Pd has caused the surface area, pore volume and pore size of TiO_2 membrane to increase significantly but still within the mesoporous level. Furthermore, the pore width distribution showed bi-modal trend where a secondary pore size emerged gradually when the Pd concentration was increased. Surface fractal analysis indicated the roughness of the TiO_2 membrane increased in the presence of Pd. According to SEM image, the membrane thickness was measured to be less than 1µm. The dominant transport mechanism for Pd-TiO_2 membrane was Knudsen diffusion and Poiseuille flow with an increment of permeability than TiO_2 membrane. This phenomena was found to be in agreement with the N_2 adsorption/desorption analysis. The permeability of H_2 and N_2 showed a significant decline when the temperature was increased from room temperature to 350^oC but increased when the pressure difference is raised. However, the permselectivity of H_2/N_2 showed a slight increment but dropped when the pressure difference was increased. The permselectivity showed gradual increment when the operating temperature was increased. In term of Pd concentration, the highest permselectivity was achieved with the addition of 10 w/w% of Pd. As a conclusion, the impregnation of Pd was able to increase H_2 permeability and permselectivity of the TiO_2 membrane.

CHAPTER 1

INTRODUCTION

1.0 Membrane Technology

According to Mulder (1996), membrane is a barrier which is selective towards substrates crossing through it from one side to another. Generally, in membrane system, there are single input stream (feed) and two output streams (retentate and permeate). A membrane process is illustrated in Figure 1.1. The feed stream contains a mixture of molecule A and B. After being subjected to a membrane, molecule B which is smaller than the pore size of the membrane tends to permeate through the membrane leaving the retentate stream enriched with molecule A. As a result, the permeate stream will mostly consist of molecule B. The product stream could be permeate or retentate depending on the process objective. If the product is in the retentate stream, the process is called removal, if otherwise enrichment. Transportation across membrane is influenced by the driving force which could be pressure difference (Al-Obaidani et al., 2008), electrical potential (Mulder, 1996), temperature (Cassano et al., 2008) and concentration (She and Hwang, 2006).

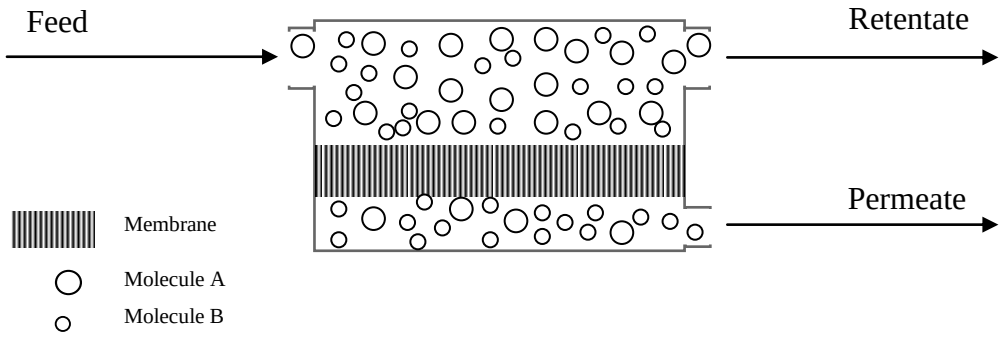

Figure 1.1 Schematic representation of membrane process

Membrane technology nowadays has become a preferential alternative in separation process due to several benefits it offers. Generally, the energy consumption is low and the process can be set to be continuous. Membrane materials can be adjusted depending on the process environment and easy to up-scale. Furthermore, it can be combined with other processes for enhanced performance (Mulder, 1996).

Membrane structure can be divided into porous and non-porous. Porous membranes are usually applied for microfiltration (MF), ultrafiltration (UF), nanofiltration (NF), reverse osmosis (RO), electrodialysis (ED), gas separation, pervaporation, membrane distillation etc. whereas the nonporous or dense membrane is used for gas purification. The porous membrane can be further classified into three categories in term of its pore size, which are macropores (> 50 nm), mesopores (2-50 nm), and micropores (<2 nm). Food and beverages, metallurgy, pulp and paper, textile, biotechnology, chemical industry, water treatment, and environment are industrial fields where membrane technology is found to be widely applied (Freeman and Pinnau, 2004).

Choice of materials used to be developed as a membrane is determined by the processing requirements, fouling tendency, chemical and thermal stability of the fields of application (Mulder, 1996). Therefore, membrane material is mainly divided into organic and inorganic. But nowadays, hybrid membranes are synthesized as well. Both of the organic and inorganic have their own advantages and disadvantage. Organic membrane is usually made of polymer materials where its long-chain of carbon content is constructed by polymerization of monomers. Examples of polymer

mostly used in the membrane fabrication are polycarbonate (Lo et al., 2009), polypropylene (Yu et al., 2009), polyehthersulfone (Susanto and Ulbricht, 2009), polyvinylidene fluoride (PVDF)(Hashim et al., 2009) etc. These polymeric membrane is widely applied and studied in fruit juice clarification (Cassano et al., 2009), water treatment (Mondal and Wickramasinghe, 2008), desalination (Cakmakci et al., 2008), gas separation (Ji et al., 2009) etc. Various techniques are discovered to fabricate a polymeric membrane such as stretching, track-etching, phase inversion, etc.

On the other hand, inorganic membranes are well known of their stability against high thermal and corrosive environment, thus, suitable for harsh industrial application. Furthermore, it also offers strong mechanical strength against structure deterioration. For this reasons, it shows a great potential to be further developed and commercialized in various applications. There are many types of inorganic membranes which are ceramic (Ha et al., 1996; Morooka et al., 1995; Ahmad et al. 2004; Gu et al., 2001) ,metal (Haag et al. 2006; Gade et al., 2009; Basile et al., 2008), glass (Shimpo et al. 2004,), carbon (Rao and Sircar, 1996; Zhiqiang et al., 2008) and zeolite (Wee et al., 2008; Nishiyama et al., 2007; Moron et al., 2002). The application varies from liquid separation to gas separation. Most inorganic membranes made of metal, carbon and zeolite are applied in hydrogen gas (H_2) purification and separation, as they possess dense or almost dense structure and provide very high selectivity. Whereas ceramic membranes that mostly possess larger pores are utilized in H_2 separation to attain higher flux. Silica (SiO_2), alumina (Al_2O_3) and titania (TiO_2) are material mostly utilized in ceramic membrane fabrication. Common fabrication techniques are sol-gel process (Xomeritakis et al.,

2009), chemical vapor deposition (CVD) (Labropoulos et al., 2009), laser synthesis (Singh et al. 2006), reversed micelle method (Ju et al, 2002), etc.

1.1 Problem Statement

H_2 has become one of important substances in the world nowadays. Its application varies from the production of synthetic ammonia and methanol, hydrogenation of organic materials, oxyhydrogen torches to rocket fuels. And today, actions have been taken to utilize this substance as primary world's driving fuel replacing the conventional fossil fuel through fuel cell technology. The use of H_2 as an alternative energy producer promises the conservation of green environment as the emission contains no CO_2. H_2 can be produced from coal, and natural gas (fossil fuels), nuclear, and biomass. The chemical and reaction process includes natural gas reforming, renewable electrolysis (water), gasification, renewable liquid reforming, nuclear high-temperature electrolysis, high-temperature thermochemical water splitting, photobiological and photoelectrochemical. More than 90% H_2 produced annually nowadays comes from steam reforming process and requires separation process to obtain desired purity of H_2 (Rand and Dell, 2008).

Currently, there are three processes for H_2 separation and purification which include pressure swing adsorption, fractional/cryogenic distillation and membrane separation. The process may be a stand-alone or the combination of the processes above (Sircar and Golden, 2000). Pressure swing adsorption makes use the advantage of gas tendency to adsorb to certain material at certain pressure. Cryogenic process is done by carrying the gas to lower temperature and separation is done by utilizing different boiling point of the substances. Although the pressure swing adsorption and

fractional/cryogenic distillation have been widely used, such systems suffer from tremendous amount of energy consumption and cost ineffective to obtain H_2 separated from other gases mixture. Membrane utilization offers competitive separation and purification capability with lower cost operation, capital investment, and ease of operation (Ockwig and Nenoff, 2007).

Since the first introduction of polysulfone fiber membranes in 1979 for the recovery of H_2 from ammonia purge gas and extraction of H_2 from petroleum cracking streams, a considerable interest to develop high-performance membranes for H_2 separation began (Mulder, 1996). Organic membranes provide acceptable performance and ease of fabrication. Current polymeric membranes commercially used for H_2 separation are made of polysulfone, polyethersulfone, ethyl cellulose etc. The H_2/CO_2 selectivity ranges from 2.5 – 3.3 at approximately 2 bar of operating pressure under 30^oC (Phair and Badwal, 2006).

However, due to their low tolerance in thermal, mechanical and chemical stability, inorganic material based membranes, with much higher stability and competitive performance are developed for industrial application. In gas separation, particularly H_2 separation, the properties (mechanical, thermal and chemical stabilities) and the performance characteristics (processability, maximum H_2 flux, permeability, selectivity, transport mechanism and lifetime) are two matters of highly concern when one want to choose the materials of membrane fabrication. For example, coal gasification operates at temperature above 1000^oC, the reforming of natural gas is run at temperature between 800-900^oC, and the water-gas shift (WGS) reaction works at 300-500^oC (Phair and Donelson, 2006). Recent researches indicate

that the inorganic membranes performance (selectivity and flux) are as competent as organic membranes (Shi et al., 1999).

Numerous studies have been conducted to find the inorganic membrane that complies with required specifications prior to commercialization for industrial and other applications. Ceramic membranes received most attention due to their lower cost and availability of easier fabrication method such as sol-gel. One of early works of sol-gel based method of developing ceramic membrane for H_2 separation was reported by de Lange et al.(1991) which is made of silica. Chai et al. (1994) has conducted work to improve the membrane permselectivity of H_2 by introducing strategic metal salts; $RuCl_3$, $Pd(NH_3)_4Cl_2$, $RhCl_3$, and H_2PtCl_6 into alumina. Attentions were also paid to the development of zirconia, its hybrid, and modified based membrane for H_2 separation (Yoshida et al., 2001; Gu et al.,2001; Fan et al.,2000)

Elemental palladium gained many attentions as it is able to dissociate H_2 into protons, let it diffused through and reassociate into H_2 again. Improvement of current palladium membrane is still being done in spite of its commercialization status. Improvement in term of thickness (Jayaraman et al., 1995), alloy (Gobina et al., 1994; Roa et al., 2003), permeability (Mejdell et al., 2008), support resistance (Zhang et al., 2007), defects and degradation (Zhang et al., 2007; Zhang et al., 2007; Wang et al., 2007), module design (Ryi et al., 2007), methods of fabrication (Kim et al., 2008; Bosko et al., 2007) have been done extensively. However, palladium drawback was the cost of the materials itself. Therefore, it is favorable to reduce the

amount used through impregnation into cheaper and abundant relevant materials such as ceramic (Uemiya et al.,1988).

Impregnation of certain materials into ceramic materials to improve the H_2 selectivity and flux, and physical properties received a lot of interest as well. Examples of materials doped for improvement were boron (Chen et al., 2001), Pd/ yttria-stabilized-zirconia (YSZ) (Tanaka et al., 2008), Pd/ Al_2O_3 (Lee et al., 1994; Ahmad and Mustafa, 2007), Pd/ SiO_2 (Gopalakrishnan et al., 2008), V-Ti-Ni (Adams and Mickalonis, 2007), Ni (Ernst et al., 2007), Ni-Ba($Zr_{0.1}Ce_{0.7}Y_{0.2}$)O_3 (Zuo et al., 2006) and etc. Based on the author best knowledge, hardly can we find works introducing TiO_2 as potential materials to be developed as H_2 separator. Kluiters (2004) stated that TiO_2 is classified as relevant materials to be developed as inorganic membrane for H_2 separation. Advantages of TiO_2 membrane is its possession of lower tortuosity, thus possibly provides higher flux (Zaspalis et al., 1992). Besides that, the TiO_2 is also considered the most chemically stable ceramic compared to others in its class such as alumina, silica and zirconia (Buekenhoudt, A, 2008).

Based on the problem listed from the ineffectiveness of polymeric membrane in harsh environment to the highly cost of palladium membrane and low selectivity of ceramic membrane, current research proposes the impregnation of elemental palladium into a ceramic membrane by sol-gel method. The usage of small amount of palladium is expected to improve the selectivity whereas the mesoporous ceramic will provide the high flux for H_2 gas across the membrane. In this work, TiO_2 is selected as the ceramic membrane as it is not only stable at elevated temperatures,

but also stable at highly acidic or alkaline environment. Furthermore, the sphere-shape crystallites of TiO_2 provides lower tortuosity to provide less resistive flow than other ceramics such as disk-shaped crystallites of γ-Al_2O_3 (Sakka, 2005).

1.2 Research Objective

There are several objectives to be achieved from this research. The objectives are;

1. To synthesize palladium-titania (Pd-TiO_2) ceramic membrane by utilizing sol-gel protocol from different formulation
2. To characterize supported and unsupported Pd-TiO_2 membrane
3. To investigate the membrane permselectivity and permeability towards H_2 and N_2 gas at various operating temperature, pressure, and concentration of impregnated Pd.

1.3 Organization of the thesis

The thesis comprises of five chapters providing all the details and findings of the research. Chapter one briefly introduces the membrane technology, characteristics of ceramic membranes, research objectives and thesis organization. Chapter two reviews all necessary literatures where it is divided into five sub-chapters. The first and second sub-chapters focuses on the latest development of TiO_2 and Pd membrane respectively with their latest method of preparation. Short explanation regarding sol-gel method is presented in the third sub-chapter. The fourth sub-chapter goes for the analysis used for unsupported membrane and its corresponding parameters. Final sub-chapter discusses the analysis conducted on

supported membrane that includes performance evaluation, transport and separation mechanism.

Chapter three is about the methodology applied to run the experiment. All details about the amount and concentration of the chemicals, experimental procedures, analysis, characterization techniques, and equipments used towards the object of study are described.

Chapter four presents the experimental results and discussion. The chapter basically is divided into seven sub-chapters. The results and discussion covers the synthesis and characterization of titania sol, unsupported and supported TiO_2 and Pd-TiO_2 membrane, and their performance evaluation. Several parameters and their influences on the membrane formation has been investigated. Certain parameters has been studied using TiO_2 membrane as the subject. The optimum values are carried forward to the synthesis and further characterization of the Pd-TiO_2 membrane. Performance evaluation covers both type of membrane for comparison study. The last chapter concludes the findings in the current work with several recommendations for improvement for future work.

CHAPTER 2

LITERATURE REVIEW

2.0 Development of TiO_2 membrane

Ceramic membranes for gas separation applications have attracted considerable attention in recent years due to their competent separation performance and intrinsic thermal stability compared to polymeric separation membranes. Ceramic membranes that are commonly used as membrane for gas separation either as support or active layer are titania (TiO_2) (Ha et al., 1996), silica (SiO_2) (Morooka et al., 1995), alumina (Al_2O_3) (Ahmad et al., 2004) and zirconia (ZrO_2) (Gu et al., 2001). The performance of a membrane depends on its permeability and permselectivity/ separation factor. As reviewed by Mottern et al. (2007), dense membranes have 100% selectivity for H_2 and O_2 and acceptable flux at high temperature. Microporus membranes (pore size <2 nm) provide less than 100% H_2 selectivity with higher flux, whereas mesoporous membranes (pore size 2-50 nm) give very high fluxes with moderate selectivity for separation of light molecules (H_2) from heavier ones (CO_2, N_2, CH_4 etc.).

TiO_2 membrane is one of the most studied materials for various applications in a form of thin film, which is also utilized in the fabrication of supported TiO_2 membrane. Aspects that one should consider in membrane development are the pore size, grain size, thickness, surface area, porosity, and performance. TiO_2 membrane possesses the highest chemical stability, in comparison to alumina, zirconia and silica (Buekenhoudt, 2008). Pure TiO_2 membranes provide competitive advantage with better fouling resistance, thus higher fluid flux due to their amphiphilic surface

properties (Wang et al., 2007). This section reviews previous works of TiO_2 membrane, morphology, its formations and reported performance.

Atmospheric pressure chemical vapor deposition (APCVD) is used in the synthesis TiO_2 membrane at different deposition temperature (250^{o}-400^{o}C) as reported by Ha et al. (1996). The selectivity (H_2/N_2) decreased from 96 to 3.9 as the deposition temperature was increased from 250 to 400^{o}C. The governed mechanism was Knudsen diffusion in which the gas mostly permeates the membrane through the pores formed in the TiO_2 crystalline and gradually decreased with an increase of temperature.

Brasseur-Tilmant et al. (2000) prepared TiO_2 membrane by hydrolytic decomposition using titanium tetra-isopropoxide in supercritical propan-2-ol. The anatase particle size deposited as film was reported to be as small as 30nm. The thickness estimation was 1-3um with penetration depth into the support was between 20-30um. The permeation selectivity from permeation measurement of H_2 and N_2 was closed to predicted value from Knudsen diffusion model.

Yu et al. (2003) reported that the formation of TiO_2 thin film as thin as 220 – 300nm deposited on silica using liquid phase deposition method (LPD). The increasing temperature of calcination led to thinner and non-uniform film, lower surface area, rutile formation, bigger crystallite size, and cracks due to extreme densification. By controlling the pH of TiO_2 solution, the deposition of film was facilitated by the electrostatic attraction between the TiO_2 solution and silica as both materials possess different isoelectric point.

TiO_2 membrane is also prepared using wet powder spraying method (Zhao et al., 2004). The calcination was performed at heating and cooling rate of 5^oC/min and dwell time of 1h in the range of 800-950^oC. However, the pore size (0.11-0.12µm) and thickness (20-30µm) were too large to be perceived of giving acceptable performance in hydrogen separation. Based on the provided XRD data, the TiO_2 was completely in rutile phase with very narrow peak at high intensity at $2\theta = 27^o$ probably due to very high calcination temperature. The reported air flux was 1.9 x 10^5 L/h m^2 bar.

A sol gel method was utilized by Shen et al. (2005) in preparing TiO_2 thin film on316L stainless steel substrate for corrosion protection. Tetra-n-butyl titanate ($Ti(O\text{-}n\text{-}Bu)_4$) was used as precursor. After calcination at 450^oC, the particle diameter ranged between 15-18 nm with thickness 370 – 375nm. The morphology of the film was porous, uniform and no cracks were detected. As reported early by Wong et al. (2003), the particle size that forms the membrane layer dictated the pore size. Their work also showed an excellent corrosion resistance of TiO_2 in chloride containing solution at room temperature.

Ding et al. (2006) found a new route in preparing TiO_2 membrane with ultrafiltration level. The nanoparticles were synthesized by a wet chemical method before being added with dispersant agent and polymeric compounds. The suspension was coated on membrane support by dip-coating. The XRD results revealed that the TiO_2 membrane was in full anatase phase. The pore diameter and minimum thickness were reported to be 60nm and 5.9µm, respectively.

Meulenberg et al. (2006) utilized wet powder spraying method (WPS) and screen printing in preparing TiO_2 membrane. The reported pore diameter and thickness were 100nm and 40 - 50µm, respectively. The air flow rate was measured to be 1.9 x 10^5 l/h m^2 bar.

A thin film of TiO_2 with thickness of 20 nm was prepared based on the use of peroxo-titanium complex as a single precursor as reported by Sankapal et al. (2005). The substrate used were glass, quartz and indium tin oxide (ITO) substrates. The crystallite size was estimated to be 16, 24 and 23 nm on ITO, glass and quartz substrates respectively. It shows that the crystal formation is influenced by the substrates used for film deposition. Because the substrates used are non-porous, it does not suffer from solution penetration and able to coat a very thin film (20 nm). The XRD indicated the TiO_2 existed in anatase phase after calcination at 500^oC for both film and powder form.

Chou et al.(1999) has synthesized TiO_2 membrane by deposition of TiO_2 colloids at different size to create multilayer. Their findings show that, multiple coatings with the same colloid size decreases the pore diameter until it reached critical thickness where the diameter eventually reached a constant. According to their work, larger colloid size led to the formation of larger pore diameter. Based on gas permeability test, the reduction of pore diameter from 1.5µm to 0.12µm only changed the permeance from 500x10^{-7} to 250x10^{-7} mol/m^2s Pa. The characteristic of unsupported membrane does not really represent the supported membrane. The author found that even though the mercury intrusion indicated a pore size of 0.03µm, the gas permeation techniques indicated a reading of 0.12µm, which show the last

coating did not completely cover the previous layer. It was also reported that, diluted slurries was easier to coat and obtain uniform layers as easier particle movement facilitated in particle filling in the pore-mouth region at the surface. Table 2.1 shows the surface roughness reported by the authors of membrane support and after successive coatings. The surface roughness is reduced after the membrane support is coated with smaller titania particles and colloids.

Table 2.1 Membrane sample and its respective measured surface roughness (Chou et al., 1999)

Sample	**Surface roughness (nm)**
Membrane support	1500
After coating with 0.5um titania particle	800
After further coating with 30nm titania colloids	550

Ge et al. (2006) utilized sol-gel method to prepare the TiO_2 thin film deposited on glass substrates by dip-coating. The film thickness was 200 nm according to SEM analysis. They utilized XRD and TEM to estimate the crystal size and particle size of the TiO_2 nanoparticles of a thin film. The results showed the particle size observed and measured under TEM observation was in agreement with the average crystal size defined from the XRD pattern. It was also reported that the smaller the crystal size, the higher the surface area of the TiO_2.

Gestel et al. (2002) synthesized binary layers of TiO_2 membrane. Intermediate layer consisted of mesoporous characteristic prepared from colloidal route of sol-gel. The top layer was microporous prepared from polymeric route of sol-gel. They reported the relationship between the crystal growth and the effects of

membrane structure. As the crystal increased in size, the surface area and pore volume showed reduction. This caused the membranes to have broad pore size distribution. The reported mean pore size of polymeric TiO_2 membrane was 1.6, 2.4 and 3.4nm at calcination temperature of 200 (Amorphous), 300 (Anatase) and 400^oC (Anatase), respectively. Another recent work by sol-gel method in synthesizing TiO_2 membrane was reported by Kermanpur et al. (2008). The membrane layer was formed by dip-coating. The size and membrane thickness was measured to be 50 nm and 2μm, respectively. The addition of diethanol-amine (DEA) into TiO_2 sol was reported to improved the coating properties of the sol from cracks particularly during critical drying and calcination procedure (Gestel et al., 2008). The thickness of the TiO_2 membrane was 50 – 100 nm facilitated by the presence of intermediate layer.

Zaspalis et al. (1992) had conducted extensive study in providing TiO_2 membrane with improved performance. They reported by adding sulphate ion (adding sulphuric acid before hydrolysis), the TiO_2 anatase structural transformation into rutile was retarded. Polyvinyl alcohol (PVA) was added to enhance the gel network strength during the drying and calcination process. Additional of hydroxyl-propyl cellulose (HPC) was added to encounter the destabilization occurred when more than 1-2%wt of PVA added into the titania sol. TiO_2 was also reported to have lower tortuosity (2.9; 3.3) than γ-alumina (4.5; 5.4) based on helium and water permeability correspondingly.

TiO_2 membrane presence also provided smoother surface in synthesizing composite Al_2O_3-SiO_2-TiO_2 (Zheng et al. 1998). Smooth surface is necessary in producing free-crack film of the top layer as its irregularities are affected by the

support surface. By utilizing TiO_2 membrane as support, one does not need to have intermediate layer to flatten the roughness surface of the support before coating with top layer. Intermediate layer must have good adhesion with both top and support layer, and as thin as possible to reduce the flow resistance (Chou et al., 1999). Gestel et al., 2002 reported that TiO_2 has better corrosion resistant at lower thermal treatment (400^oC) than alumina (1200^oC). They also claimed that TiO_2 interlayer (double dip-coating) was a preferable due to higher chemical stability, smaller pore size and narrow pore size distribution.

2.1 Development of Palladium (Pd) based membrane

Palladium and palladium alloys are able to separate hydrogen at highest selectivity because of the high solubility and diffusivity of the gas in their lattice. As a nonporous membrane, the hydrogen transport mechanism through palladium membranes is due to the interaction of hydrogen atoms and palladium metal. Molecular hydrogen is dissociated and chemisorbed on one side of the membrane surface and dissolved in the palladium matrix. The atomic hydrogen then diffuses to the other side of the membrane surface. The driving force for the permeation is the difference in the square root of the hydrogen partial pressure on both sides of the membrane. The experimental evidence shows that only hydrogen can permeate through the dense film of palladium-based membranes, whereas no other gas molecules are allowed to transfer through it (Angelo et al.,2008).

Besides being imminent permeable to hydrogen, it is also catalytically active toward many hydrogen-involving reactions, thus it offers great economic opportunities than platinum in term of significant cost reduction. At high

temperatures, the palladium capability increases exponentially to cope up with adsorbing hydrogen 900 times of its own volume. For this reason, it is used in hydrogen gas purification and separation with high selectivity (Othman and Kim, 2008).

In the case of membrane, where the palladium made as a thin film sheet, the hydrogenated substance is adsorbed on the surface resulting the atomic hydrogen penetrates through it (Gryaznov, 1986). However, thin palladium sheet may suffer easily from mechanical damage due to its embrittlement from the repeating hydrogen sorption and desorption process. Alloy palladium was suggested by Gryaznov, (1986) to improve the durability. Cheng and co-workers (2002) experimented Pd-Ag and palladium thin sheet of electroless plating technique for hydrogen separation. The result was high purity hydrogen. Palladium-doped zeolite composite membranes was prepared by Moron et al.(2002). Chen et al. (2003) had developed a highly metal-dispersion Pd/Alumina composite membrane. The technique used was wetness-impregnation. The permeation test showed the separation factor of 3.74 for H_2/N_2 system which is slightly above Knudsen value. Under the same concept, Ahmad et al (2007) also synthesized highly dispersed palladium within alumina membrane for hydrogen separation by sol gel method but no performance being reported. Roa et al.(2003) introduced the composite membrane consisting palladium and copper by successive electroless deposition of Pd and Cu. The hydrogen flux of 1 μm thick Pd-Cu film was 0.8 mol/m^2s at 450^{o}C with H_2/N_2 selectivity to be 1150 at 3.5 bar. Palladium was also utilized to construct tubular catalytic membrane (TCM) to directly synthesis H_2O_2 from hydrogen and oxygen gas. The preparation method

involved deposition-precipitation and electroless plating deposition (Abate et al., 2005).

Tanaka workgroups have developed a composite membrane consisting palladium metal, yttria-stabilized zirconia (YSZ) and γ-alumina (Tanaka et al., 2008). The basic preparation consisted of sol mixing between the nano-size YSZ and boehmite sol. The palladium impregnation was done by vacuum-assisted electroless plating. The membrane flux increased corresponding to the increase of transmembrane pressure and temperature. The reported hydrogen permeance was approximately 1.95×10^{-6} mol $m^{-2}s^{-1}Pa^{-1}$ but decreased by time showing instability of the membrane structure at 500-600^{o}C. It was reported that the decline was due to the agglomeration of palladium particles impregnated in the pore network at elevated temperature.

2.2 Sol-gel and membrane formation

Generally, there are two main paths in synthesizing ceramic membranes: sol-gel modification and CVD. The latter method requires large capital investment and complicated design and settings for controlled conditions of deposition (Wu and Cheng, 2000). Sol-gel method offers wide range of flexibility in term of porosity and pore size. By having the advantages of controlling these two prominent factors, the permeability and selectivity can be adjusted through parameters of the sol synthesis itself such as temperature and concentration. Besides, sol-gel method is the best alternative for new material fabrication due to high homogeneity, flexibility in controlling parameters, the possibility of coating on substrates with large areas and low in cost (Lee et al. 1997). Other advantages of sol-gel are:

1. Simple and attractive method to synthesis mesoporous and microporous level for both inert or catalytically active membranes
2. Addition of active metal precursors at sol stage allows highly dispersed catalytic sites
3. It allows the preparation of single or mixed oxide
4. Multilayer deposition and controlled structures with well defined composition and activity can be done straightforwardly

In sol-gel based membrane fabrication, the gels deposited as layer can either be polymeric gel or physical gel. Polymeric gel uses organic solution as it media to form in which the relative rates and extents of chemical reactions lead to cluster polymerization and interpenetration. This type of gel leads to the formation of microporous or almost dense top-layers. Compared to the polymeric route, the physical or colloidal gel is synthesized through aqueous media dealing with steric and electric effects between the colloids. The final gel formed would be mesoporous and microporous top layers. The dried gels of both types are known as xerogel or an aerogel, based on the drying method employed (Pierre, 1998). Figure 2.1 shows synthesis routes of both gels.

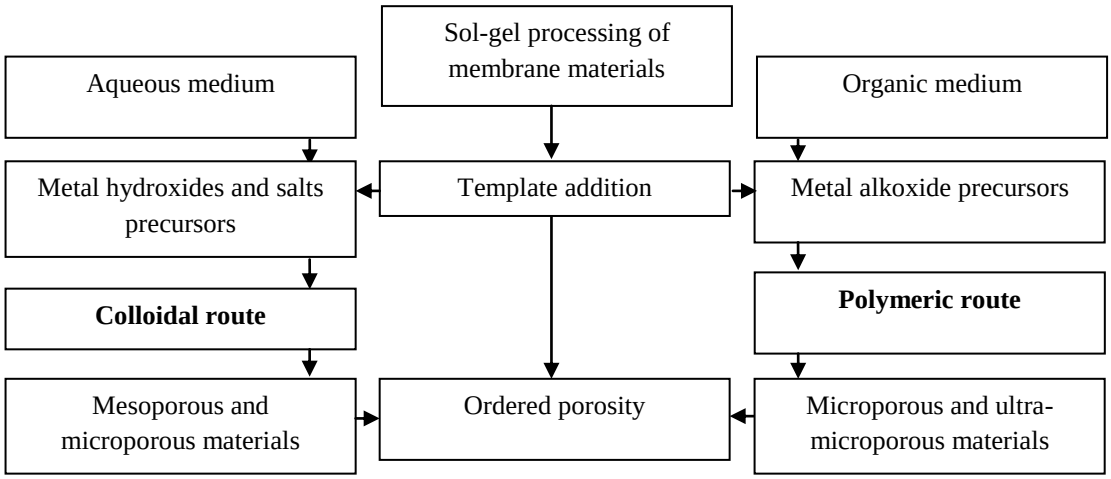

Figure 2.1 Schematic flow diagram of colloidal and polymeric routes in sol-gel process (Pierre, 1998)

TiO_2 sol can also be prepared either through the colloidal route or polymeric route. It was the same concept applied in sol-gel method to produce oxide materials. Both routes engage hydrolysis of alkoxide, peptization of hydrous oxide of titanium in obtaining sol, adjustment of the sol viscosity by including binder and other additives, filtration of the viscous sol through a microporous support, gelation and calcination at the desired temperature. The hydrolysis of alkoxide precursors induces condensation and inorganic polymerization. For TiO_2 sol, the alkoxide may be titanium-isopropoxide (Zaspalis et al., 1992, Zhang et al., 2007), titanyl iso-butoxide, titanium tetrabutoxide (Seshadri et al. 2003), titanium sulfate (Wang et al. 2007), titanium tetrachloride (Ding et al., 2006) etc.

The colloidal route involves the reaction between the alkoxide precursor and a large excess water which is called hydrolysis. The peptization process afterwards is highly influenced by its processing conditions such as pH, molar ratio between the precursor and acid, and temperatures affect the final particle size of the colloid. An